Journal of Organometallic Chemistry 897 (2019) 200–206

Contents lists available at ScienceDirect

Journal of Organometallic Chemistry

journal homepage: www.elsevier.com/locate/jorganchem

Synthesis, characterization and catalytic activity of supported vanadium Schiff base complex as a magnetically recoverable nanocatalyst in epoxidation of alkenes and oxidation of sulfides

Mojtaba Bagherzadeh*, Mohammad Bahjati, Anahita Mortazavi-Manesh

Chemistry Department, Sharif University of Technology, Tehran, P.O. Box 11155-3615, Iran

ARTICLE INFO

Article history:
Received 9 April 2019
Received in revised form
16 June 2019
Accepted 28 June 2019
Available online 9 July 2019

Keywords:
Vanadyl acetylacetonate
Magnetic nanocatalyst
Oxidation
Alkenes
Sulfides

ABSTRACT

A new magnetically separable nanocatalyst was successfully synthesized by immobilizing of vanadyl acetylacetonate complex, $[VO(acac)_2]$, onto silica coated magnetite nanoparticles previously functionalized with 3-aminopropyltriethoxysilane (3-APTES) and reacted by 5-bromosalicylaldehyde to form Schiff base moiety. The obtained nanocatalyst was characterized by elemental analysis (CHN), FT-IR spectroscopy, Powder X-ray diffraction (XRD), field emission scanning electron microscopy (FE-SEM), inductively coupled plasma optical emission spectrometry (ICP-OES) and thermogravimetric analysis (TGA). Eventually, the resulting nanoparticles were used as catalyst for epoxidation of alkenes and oxidation of sulfides using *tert*-butyl hydroperoxide (TBHP) as an oxidant.

1. Introduction

Nowadays, because of the importance of environmental and economic issues, global scientific and industrial discoveries in the field of catalysts should use the principles of "Green Chemistry" [1–5]. Recovery and reusability are the two valuable keys after catalytic reactions for the definition of sustainability and will show that a catalytic process follows the "Green Chemistry" principles [6,7]. But in practical applications, using homogeneous catalysts in a real catalytic system has the basic problems: high cost, time-consuming and boring procedure for the catalyst separation and recovery [2,8,9]. One way to solve these problems is heterogenization of homogeneous catalysts on solid supports like polymers, zeolites and metal oxides [6,10–12]. Among various solid supports, magnetic nanoparticles (MNPs) have revolutionized in the field of catalysts due to their unique properties especially simple separation from the reaction mixture. Supported catalysts on magnetic nanoparticles can be quickly separated from the reaction mixture by inducing a magnetic field and can be reused for the next time [13–17].

According to attractive properties of magnetic nanoparticles, they have found application in various fields, from medical and biology to material science and catalyst. When the magnetic particles become smaller and smaller, increasing the surface area and surface-to-volume ratio of these particles causes lots of the catalytically active structures can be loaded onto the surface and this high loading increases the activity of catalytic transformations. On the other hand, when the particles become small, they are easily dispersible in solvents, as a result, access to the catalytically active sites is more comfortable [6,18]. However, uncoated magnetic nanoparticles have the tendency to agglomeration. To overcome this drawback, magnetic nanoparticles coated by protective agents like silica, alumina, ceria, titania, polymers and other capping agents. Also, this strategy provides convenient and practical way to immobilize metal complexes on the surface of magnetite nanoparticles [15,19–21].

In this paper, we report the multistep preparation of a new magnetically separable nanocatalyst as the recyclable catalyst for epoxidation of alkenes and oxidation of sulfides by immobilizing of $[VO(acac)_2]$ onto the surface of the modified magnetite nanoparticles. The prepared nanocatalyst can be easily separated from the reaction mixture with an external magnet and storage for the next reaction.

* Corresponding author.
E-mail address: bagherzadeh@sharif.edu (M. Bagherzadeh).

https://doi.org/10.1016/j.jorganchem.2019.06.036
0022-328X/

2. Experimental

2.1. Materials and methods

All chemical materials and solvents were purchased from chemical companies, Fluka, Merck and Sigma-Aldrich.

Elemental analysis (CHN) was obtained from a Thermo Finnigan Model FlashEA 1112 series analyzer. Fourier transform infrared (FT-IR) spectra were recorded on a ABB Bomem MB-100 spectrometer using a KBr pellet for sample preparation. Powder X-ray diffraction (PXRD) peaks were collected with a Bruker diffractometer (D4 ENDEAVOR) with Cu Kα as a radiation source ($\lambda = 0.15406$ nm, 40 kV, 40 mA). Field emission scanning electron micrograph (FE-SEM) performed on a TESCAN MIRA II for determining the morphology of the obtained nanoparticles. Metal content of the prepared nanocatalyst was determined by inductively coupled plasma optical emission spectrometery (ICP-OES) performed on a Varian 730-ES spectrometer. Gas chromatographic (GC) analyses were carried out on an Agilent Technologies 6890 N, including a 19091J-236 HP-5,5% phenyl methyl siloxane, capillary column (60.0 m × 250 μm × 1.00 μm). Thermogravimetric analysis (TGA) were accomplished by METTLER TOLEDO TGA/DSC.

2.2. Synthesis of Fe_3O_4 nanoparticles (MNPs)

The Fe_3O_4 nanoparticles were prepared by co-precipitation method [22]. The amount of 5.2 g (19.3 mmol) of $FeCl_3 \cdot 6H_2O$ and 2 g (10.0 mmol) of $FeCl_2 \cdot 4H_2O$ were dissolved in 100 mL distilled water under Argon atmosphere. Then, 20 mL of the 25%.NH_3 solution was added dropwise into the precursor solution and the reaction mixture was vigorously stirred for 30 min at room temperature. The formed black magnetite precipitates were separated with a magnet and rinsed several times with distilled water and dried in oven at 80 °C for 24 h.

2.3. Synthesis of silica-coated magnetite nanoparticles (SMNPs)

Silica coating of the prepared Fe_3O_4 nanoparticles was the next step. The amount of one gram of the prepared Fe_3O_4 nanoparticles was added into 40 mL of ethanol and 10 mL of distilled water and dispersed by ultrasonic. After dispersion, 2 mL of tetraethylorthosilicate (TEOS) was added into the suspension and it was allowed to stir for 30 min at 40 °C. Eventually, the pH of the reaction mixture was increased with ammonia to pH = 10 and the mixture was stirred at 40 °C for 24 h. The dark brown silica coated magnetite nanoparticles (SMNPs) were separated with a magnet and rinsed with distilled water and ethanol and dried in oven at 70 °C for 24 h.

2.4. Synthesis of amino-functionalized silica-coated magnetite nanoparticles (ASMNPs)

For attaining the amino-functionalized silica-coated magnetite nanoparticle (ASMNPs), 2.5 mL of 3-aminopropyltriethoxysilane (3-APTES) dissolved in 50 mL of ethanol and was added dropwise to the suspension of 0.5 g of the SMNPs in 50 ml of distilled water. Then, with using KOH, the pH value of the reaction mixture was increased to pH = 11 and the reaction mixture was stirred at 70 °C for 5 h. Eventually, the dark brown ASMNPs were collected using a magnet and obtained precipitates were rinsed several times with distilled water and dried in oven at 70 °C for 24 h.

2.5. Synthesis of Schiff base functionalized silica-coated magnetite nanoparticles (Sb@SMNPs)

The reaction between amino group of the ASMNPs and carbonyl group of the 5-bromosalicylaldehyde was carried out via Schiff base condensation reaction. The amount of 0.5 g of the prepared ASMNPs and 0.2 g (1.0 mmol) of 5-bromosalicylaldehyde were added in to 50 mL of ethanol and the mixture was refluxed with continuous stirring for 24 h. The obtained nanoparticles were separated with a magnet, rinsed several times with ethanol and dried in oven at 70 °C for 24 h.

2.6. Immobilization of $VO(acac)_2$ onto Sb@SMNPs

To immobilize the oxo-vanadium complex onto Sb@SMNPs, commercially available $VO(acac)_2$ was used as precursor. The amount of 0.2 g (0.75 mmol) of $VO(acac)_2$ and 0.1 g of the prepared Sb@SMNPs were added into 10 mL of methanol and the mixture was vigorously stirred and refluxed for 24 h. The obtained nanoparticles were separated with a magnet, rinsed several times with methanol and dried in oven at 70 °C for 24 h. Formation of the obtained product was corroborated by FT-IR.

2.7. General procedure for epoxidation of alkenes and oxidation of sulfides

In a typical run, nanocatalyst (1 mg, 0.51×10^{-3} mmol), substrate (0.2 mmol) and *tert*-Butyl hydroperoxide (0.6 mmol) were added into 1 mL of 1,2-dichloroethane (DCE) in a tube. Then, the mixture was stirred vigorously at 85 °C. At the end of each reaction, the nanocatalysts were collected using a magnet, rinsed several times with DCE, dried under in oven and reused. Formation of products and consumption of substrates were monitored by gas chromatography (GC).

2.8. Reusability of the nanocatalyst

For determining the reusability and sustainability of the prepared nanocatalyst, at the end of each reaction, the nanocatalyst was separated from the reaction mixture with a magnet, washed several times with DCE and dried in room temperature for 24 h.

3. Results and discussion

3.1. Characterization

3.1.1. FT-IR spectroscopy

The preparation of product in each step was confirmed by FT-IR spectroscopy. Fig. 1 shows the FT-IR spectra of MNPs, SMNPs, ASMNPs, Sb@SMNPs and VO(acac)@Sb@SMNPs in the range of 400–4000 cm^{-1}. Fig. 1a indicates a peak at 590 cm^{-1} due to the Fe-O stretching vibration and a broad peak at 3435 cm^{-1} is associated to the stretching vibration of surface hydroxyl groups. In Fig. 1b, the silica coating of the MNPs was corroborated by peaks at 806 cm^{-1} and 1103 cm^{-1} which attributed to the Si-O-Si symmetric and Si-O-Si asymmetric stretching bands, respectively. The FT-IR spectra of Fe_3O_4@SiO_2-NH_2 depicts a doublet peak at 2870 cm^{-1} and 2935 cm^{-1} corresponding to symmetric and asymmetric stretching modes of -CH_2 groups, respectively (Fig. 1c). In Fig. 1d, after the reaction between ASMNPs and 5-bromosalicylaldehyde, the product shows a peak at 1643 cm^{-1} which assigned to imine group. In comparison with Sb@SMNPs (Fig. 1d), it is observed that the peak at 1643 cm^{-1} shifted to 1630 cm^{-1} due to the covalent binding of the Sb@SMNPs to the metal center and confirms that anchoring of vanadium was successfully completed onto the surface of Sb@SMNPs (Fig. 1e).

3.1.2. X-ray diffraction studies (XRD)

To study the crystalline structure of the prepared nanocatalyst,

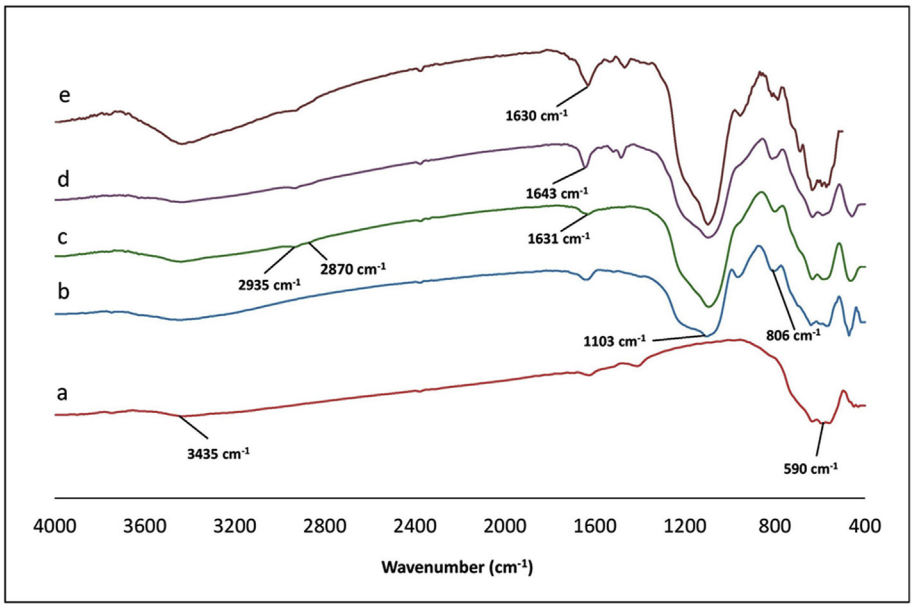

Fig. 1. FT-IR Spectra of a) MNPs; b) SMNPs; c) ASMNPs; d) Sb@SMNPs and e) VO(acac)@Sb@SMNPs

XRD analysis was carried out. In Fig. 2, the XRD pattern of the prepared nanocatalyst involves of six characteristic peaks ($2\theta = 30.26^\circ$, 35.62°, 43.3°, 53.6°, 57.25° and 62.9°) corresponding to (220), (311), (400), (422), (511) and (440) brag reflection, respectively. These diffraction peaks are consistent with the database in JCPDS file (JCPDS no. 19-0629) assigned to the planes of inverse cubic spinel structured Fe_3O_4 [23–25]. Also, Fig. 2b shows the XRD pattern of the nanocatalyst after 7th catalytic reaction cycle. The same characteristic peaks can also be found in this pattern suggesting that the crystalline structure of Fe_3O_4 nanoparticles does not change after 7th reaction run.

3.1.3. FE-SEM and EDX analysis

The morphological and structural properties of the nanoparticles were studied by FE-SEM. Fig. 3 shows the FE-SEM image of the prepared nanoparticles. As shown in the image, the nanoparticles have a spherical shape with particle diameter between 30 and 50 nm. Also, EDX analysis (Fig. 4), corroborated the presence of vanadium in the obtained nanoparticles. In addition, the vanadium content of the nanoparticle was found to be 0.51 mmol g^{-1} by using ICP-OES technique. Based on the nitrogen content (0.8% N, 0.57 mmol g^{-1}) determined by elemental analysis (CHN), the molar ratio of the Schiff base and vanadium in the synthesized nanocatalyst is nearly 1:1 which agreement with

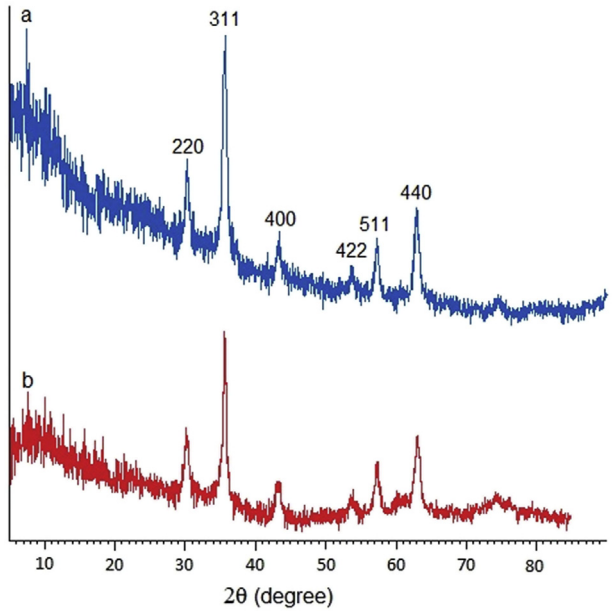

Fig. 2. XRD pattern of fresh (a) and used (b) nanocatalyst after 7th reaction cycle.

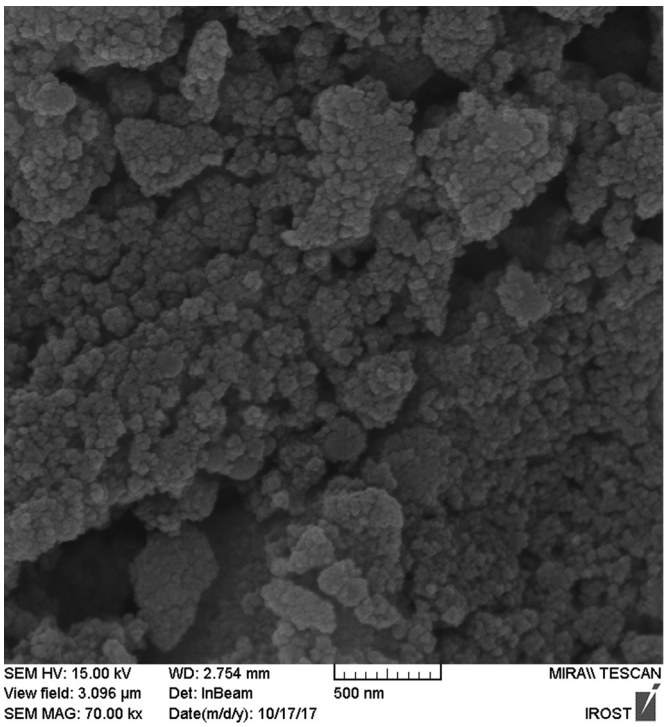

Fig. 3. FE-SEM image of VO(acac)@Sb@SMNPs

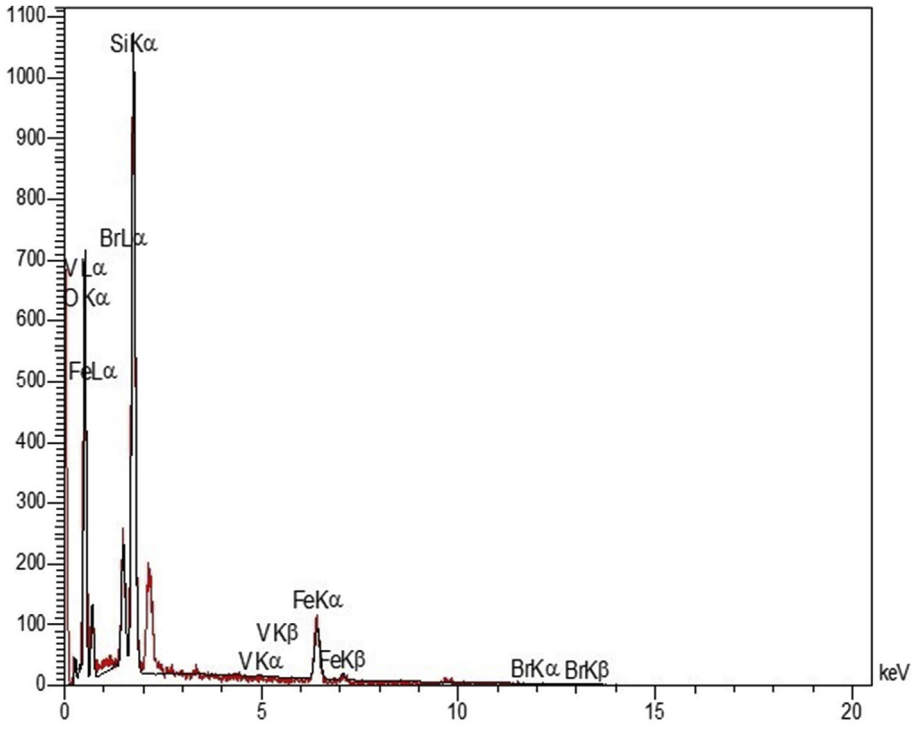

Fig. 4. EDX analysis of VO(acac)@Sb@SMNPs

structure it has been shown in Scheme 1.

3.1.4. Thermogravimetric analysis (TGA)

The thermal stability of the nanocatalyst was evaluated by TGA and resulting thermogram depicted in Fig. 5. The TG curve of the VO(acac)@Sb@SMNPs exhibited three mass losses in the range of 25–800 °C. The first weight loss (3.8%) between 25 and 205 °C arising from the fact that physically adsorbed water was evaporated. The second and third weight loss (3.3% and 2.06%, respectively) between 205 °C and 800 °C ascribe to the loss of organic groups.

3.2. Catalytic studies

Vanadium compounds have attracted much attention because they have widely been used for homogeneous, heterogeneous and industrial oxidation processes [26–29]. In this way, catalytic performance of the prepared nanocatalyst was investigated in the epoxidation of alkenes and oxidation of sulfides.

In order to find best reaction condition, we used cyclooctene as a model. To find the best oxidant for this reaction, under same temperature and reaction time, different oxidants such as TBHP, H_2O_2 and UHP (urea-hydrogen peroxide) were examined and finally TBHP was found to be the best oxidant for the epoxidation of cyclooctene (Table 1).

Different amounts of the nanocatalyst were used (Table 2, entries 1-5) and results show that increasing the catalyst amount from 0.51×10^{-3} to 2.55×10^{-3} mmol did not significantly affect the conversion. Among various quantity of the substrate/oxidant ratio (entries 1, 6-8), the ratio 1:3 for substrate and oxidant was concluded. Effect of solvent on the catalytic activity was studied by using some of solvents (entries 1, 9-13). Due to the competition

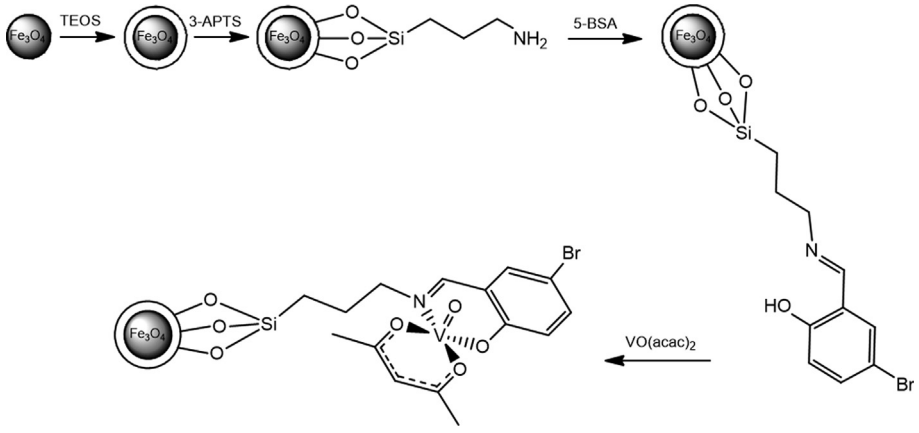

Scheme 1. Step-by-step synthesis of the VO(acac)@Sb@SMNPs nanocatalyst.

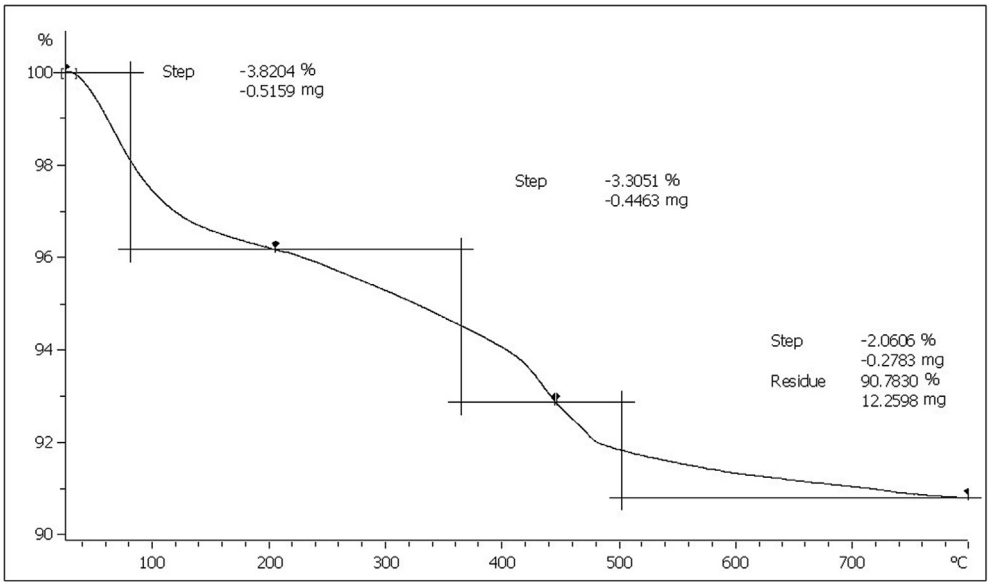

Fig. 5. TGA curve of VO(acac)@Sb@SMNPs

Table 1
Epoxidation of cyclooctene with different oxidants in presence of VO(acac)Sb@SMNPs[a]

Entry	Catalyst (mmol)	Oxidant	Conversion (%)[b]	Selectivity (%)[c]	TON[d]
1	0.51×10^{-3}	H_2O_2	———————	———————	–
			(10)[e]	(100)[e]	(39)[e]
2	0.51×10^{-3}	UHP	Trace	100	4
3	0.51×10^{-3}	TBHP	55	100	216

[a] Reaction conditions: cyclooctene (0.2 mmol), oxidant (0.2 mmol), catalyst (1 mg, 0.51×10^{-3} mmol), $C_2H_4Cl_2$ (1 mL), reaction time: 7 h and 85 °C.
[b] GC conversion based on starting alkene.
[c] Selectivity to epoxide = ((epoxide)/(epoxide + other products)) × 100.
[d] TON = (mmol of product)/(mmol of catalyst).
[e] Values in parentheses were obtained in the presence of acetonitrile as solvent.

Table 2
Effect of the catalyst amount, TBHP amount, various solvents and temperature on the epoxidation of cyclooctene with VO(acac)@Sb@SMNPs.[a]

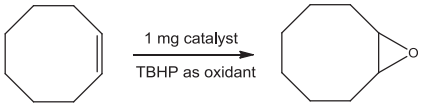

Entry	Catalyst (mmol)	Oxidant (mmol)	Solvent	Temperature (°C)	Conversion (%)[b]	Selectivity (%)[c]	TON[d]
1	0.51×10^{-3}	0.6	DCE	85	88	100	345
2	1.02×10^{-3}	0.6	DCE	85	90	100	176
3	1.53×10^{-3}	0.6	DCE	85	91	100	119
4	2.04×10^{-3}	0.6	DCE	85	91	100	89
5	2.55×10^{-3}	0.6	DCE	85	92	100	72
6	0.51×10^{-3}	0.2	DCE	85	55	100	216
7	0.51×10^{-3}	0.4	DCE	85	84	100	329
8	0.51×10^{-3}	0.8	DCE	85	86	100	337
9	0.51×10^{-3}	0.6	Ethanol	85	29	100	114
10	0.51×10^{-3}	0.6	Methanol	85	40	100	159
11	0.51×10^{-3}	0.6	Acetonitrile	85	19	100	75
12	0.51×10^{-3}	0.6	Chloroform	85	82	100	322
13	0.51×10^{-3}	0.6	n-Hexane	85	53	100	208
14	0.51×10^{-3}	0.6	DCE	70	44	100	173
15	0.51×10^{-3}	0.6	DCE	60	30	100	118
16	0.51×10^{-3}	0.6	DCE	r.t.	24	100	94

[a] Reaction conditions: cis-cyclooctene (0.2 mmol), $C_2H_4Cl_2$ (1 ml), reaction time: 7 h.
[b] GC conversions based on starting alkenes.
[c] Selectivity to epoxide= ((epoxide)/(epoxide + other products)) × 100.
[d] TON = (mmol of product)/(mmol of catalyst).

Table 3
Catalytic epoxidation of different alkenes in the presence of VO(acac)@Sb@SMNPs.[a]

Entry	Substrate	Time (h)	Conversion (%)[b]	Selectivity (%)[c]	TON[d]
1	Cyclooctene	7	88	>99	345
2	Styrene	7	94	55	369
3	4-methyl styrene	7	95	48	373
4	4-methoxy styrene	9	76	76	298
5	α-methyl styrene	9	91	95	357
6	Cis stilbene	7	56	47	220
7	Trans stilbene	7	61	50	239
8	1-octene	9	40	42	157
9	Trans 2-octene	9	67	54	263

[a] Reaction conditions: substrate (0.2 mmol), TBHP (0.6 mmol), catalyst (0.51×10^{-3} mmol), $C_2H_4Cl_2$ (1 ml) and 85 °C.
[b] GC conversions based on starting alkenes.
[c] Selectivity to epoxide= ((epoxide)/(epoxide + other products)) × 100.
[d] TON = (mmol of product)/(mmol of catalyst).

between solvents with TBHP for coordination to the vanadium center, non-coordinating solvents such as 1,2-dichloroethane, chloroform and n-hexane were exhibited high conversion than coordinating solvents (ethanol, methanol and acetonitrile). After finding out the best solvent (DCE), different temperatures were tested (entries 1, 14-16) and 85 °C was found to be the best reaction temperature.

Under optimized reaction conditions, epoxidation of some alkene was evaluated (Table 3). Cyclooctene as an example for cyclic alkene showed notable conversion and selectivity (entry 1). For styrene and its derivatives (entries 2-5), α-methylstyrene showed significant selectivity. Cis stilbene and trans stilbene showed conversion and selectivity close to each other (entries 6-7). In linear substrates such as 1-octene and *trans*-2-octene (entries 8-9), *trans*-2-octene showed high conversion and selectivity than 1-octene which indicates that internal carbon double bond more active than terminal carbon double bond.

Also, under optimization condition that found for epoxidation of alkenes, oxidation of some sulfide to corresponding sulfoxide was studied (Table 4). The results show that oxidation of sulfides to corresponding sulfoxides exhibited excellent selectivity and conversion after 1 h.

3.2.1. Reusability

Catalyst stability and reusability are two great importance parameters for identifying heterogeneous catalytic systems. To

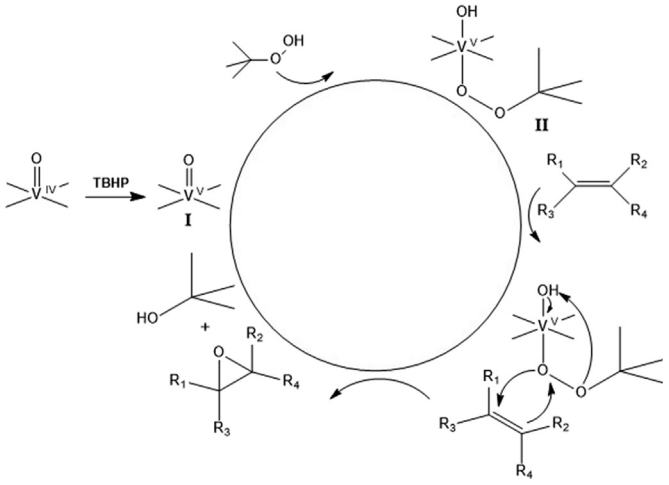

Fig. 7. The proposed mechanism for epoxidation of alkenes with VO(acac)@Sb@SMNPs

Table 4
Catalytic oxidation of different sulfides in presence of VO(acac)@Sb@SMNPs.[a]

Entry	Substrate	Time (h)	Conversion (%)[b]	Selectivity (%)[c]	TON[d]
1	Methyl phenyl sulfide	1	100	100	392
2	Diallyl sulfide	1	88	100	345
3	Diphenyl sulfide	1	71	100	278
4	Dibuthyl sulfide	1	100	100	392
5	Benzyl phenyl sulfide	1	64	100	251

[a] Reaction conditions: substrate (0.2 mmol), TBHP (0.6 mmol), catalyst (0.51×10^{-3} mmol), $C_2H_4Cl_2$ (1 ml) and 85 °C.
[b] GC conversions based on starting sulfides.
[c] Selectivity to sulfoxide= ((sulfoxide)/(sulfoxide + sulfone)) × 100.
[d] TON = (mmol of product)/(mmol of catalyst).

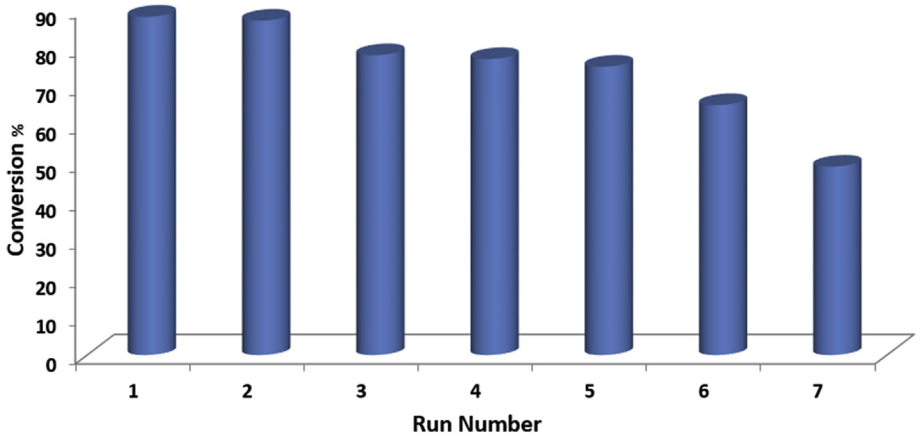

Fig. 6. Reusability of the nanocatalyst in the epoxidation of cyclooctene. Reaction conditions: cyclooctene (0.2 mmol), TBHP in water (0.6 mmol), catalyst (1.0 mg), $C_2H_4Cl_2$ (1 mL), 85 °C and 7 h reaction.

Table 5
Comparison of this work with other published works for the cyclooctene epoxidation.

Entry	Catalyst	Oxidant	Time (h)	Conversion (%)	Ref.
1	VO(acac)Sb@SMNPs	TBHP (70% aq)	7	88	This work
2	VO(Sal-Tryp)/AmpSCMNPs	TBHP	8	50	[31]
3	VO(Sal-His)/AmpSCMNPs	TBHP	8	70	[31]
4	Fe3O4@SiO2@ PTMS @Mel-Naph-VO	TBHP	8	80	[32]
5	V-MCM-41	TBHP (70% aq)	24	90	[33]

examine the stability and reusability of the nanocatalyst, at the end of each reaction, catalyst was collected with a magnet, rinsed several times with DCE and dried for 24 h. Epoxidation of cyclooctene was chosen as a model substrate to study the reusability of the synthesized nanocatalyst. Results were shown in Fig. 6. For determining catalyst leaching, after seven run, vanadium content was analyzed by ICP-OES that shows some vanadium moieties were separated from the surface of Sb@SMNPs. The catalyst was consecutively reused about six times without significant loss of activity. It should be mentioned that the decrease of catalytic efficiency after reusing for six runs may be due to release of surface-adsorbed or loosely coordinated $VO(acac)_2$ complex.

3.2.2. Proposed mechanism

According to the previous studies which were investigated by Conte et al., the accepted mechanism for epoxidation of alkenes by oxovanadium catalysts in the presence of TBHP was illustrated in Fig. 7 [30]. At first, intermediate I (oxovanadium (V)) formed by oxidation of oxovanadium (IV) with TBHP. Afterward, by simultaneously proton transfer from TBHP to V=O group, TBHP is coordinated to the metal center which acts as a Lewis acid to form the intermediate II. Eventually, interaction between the intermediate II and the alkene, causes formation of the final products, epoxy compound and t-BuOH. Also, to confirm the proposed mechanism, the epoxidation reaction of cyclooctene was controlled in the presence of hydroquinone as the radical trap and results showed that there was no change in the activity of the nanocatalyst for this reaction.

Finally, we compared the performance of VO(acac)Sb@SMNPs in the epoxidation of alkenes with other published works (Table 5). Based on these results, catalytic epoxidation of alkenes and oxidation of sulfides in the presence of VO(acac)Sb@SMNPs were preferable from the point of view of time, solvent, oxidant and amount of catalyst.

4. Conclusions

In brief, we have synthesized a new magnetically recoverable nanocatalyst by immobilization of $VO(acac)_2$ onto surface of modified silica-coated magnetite nanoparticles. The prepared nanocatalyst has been characterized by several techniques such as FT-IR, elemental analysis (CHN), XRD, ICP-OES, FE-SEM and TGA. The synthesized nanoparticles used as the catalyst for epoxidation of alkenes and oxidation of sulfides using TBHP as the oxidant and 1,2-dichloroethane as the solvent. Results showed that catalytic epoxidation of alkenes to corresponding epoxides in the presence of VO(acac)Sb@SMNPs is notable. Also, oxidation of sulfides in the optimum condition that found for epoxidation of alkenes showed excellent conversion and selectivity. Easy separation and recovery from the reaction mixture only with a magnet are other plus points of using this nanocatalyst in the consecutive runs that have a significant role in the field of catalysis.

Acknowledgments

Financial assistance from Sharif University of Technology is acknowledged.

References

[1] V. Polshettiwar, R.S. Varma, Green Chem. 12 (2010) 743–754.
[2] V. Polshettiwar, R. Luque, A. Fihri, H. Zhu, M. Bouhrara, J.M. Basset, Chem. Rev. 111 (2011) 3036.
[3] P.J. Dunn, Chem. Soc. Rev. 41 (2012) 1452–1461.
[4] R.A. Sheldon, Chem. Soc. Rev. 41 (2012) 1437–1451.
[5] P. Anastas, N. Eghbali, Chem. Soc. Rev. 39 (2010) 301–312.
[6] S. Shylesh, V. Schünemann, W.R. Thiel, Angew. Chem. Int. Ed. 49 (2010) 3428–3459.
[7] A.S. Roy, J. Mondal, B. Banerjee, P. Mondal, A. Bhaumik, S.M. Islam, Appl. Catal. A Gen. 469 (2014) 320–327.
[8] H. Keypour, M. Balali, M.M. Haghdoost, M. Bagherzadeh, RSC Adv. 5 (2015) 53349–53356.
[9] J. Govan, Y. Gun'ko, Nanomaterials 4 (2014) 222–241.
[10] A.E.C. Collis, I.T. Horváth, Catal. Sci. Technol. 1 (2011) 912–919.
[11] L.M. Rossi, N.J.S. Costa, F.P. Silva, R. Wojcieszak, Green Chem. 16 (2014) 2906–2933.
[12] S. Verma, M. Aila, S. Kaul, S.L. Jain, RSC Adv. 4 (2014) 30598–30604.
[13] M. Bagherzadeh, A. Mortazavi-Manesh, J. Coord. Chem. 68 (2015) 2347–2360.
[14] R.K. Sharma, R. Gaur, M. Yadav, A. Goswami, R. Zbořil, M.B. Gawande, Sci. Rep. 8 (2018) 1–12.
[15] M. Bagherzadeh, A. Mortazavi-Manesh, RSC Adv. 6 (2016) 41551–41560.
[16] M.B. Gawande, R. Luque, R. Zboril, ChemCatChem 6 (2014) 3312–3313.
[17] R.K. Sharma, S. Dutta, S. Sharma, R. Zboril, R.S. Varma, M.B. Gawande, Green Chem. 18 (2016) 3184–3209.
[18] H. Keypour, M. Balali, R. Nejat, M. Bagherzadeh, Appl. Organomet. Chem. 31 (2017) 1–7.
[19] J. Sun, G. Yu, L. Liu, Z. Li, Q. Kan, Q. Huo, J. Guan, Catal. Sci. Technol. 4 (2014) 1246–1252.
[20] M. Shokouhimehr, Y. Piao, J. Kim, Y. Jang, T. Hyeon, Angew. Chem. Int. Ed. 46 (2007) 7039–7043.
[21] M.B. Gawande, B. Manoj, Y. Monga, R. Zboril, R.K. Sharma, Coord. Chem. Rev. 288 (2015) 118–143.
[22] X. Liu, Z. Ma, J. Xing, H. Liu, J. Magn. Magn. Mater. 270 (2004) 1–6.
[23] J. Zheng, Y. Dong, W. Wang, Y. Ma, J. Hu, X. Chen, X. Chen, Nanoscale 5 (2013) 4894–4901.
[24] Z. Azarkamanzad, F. Farzaneh, M. Maghami, J. Simpson, M. Azarkish, Appl. Organomet. Chem. 32 (2018) 1–14.
[25] L. Hadian-Dehkordi, H. Hosseini-Monfared, Green Chem. 18 (2016) 497–507.
[26] P. Schwendt, J. Tatiersky, L. Krivosudsky, M. Šimunekova, Coord. Chem. Rev. 318 (2016) 135–140.
[27] H. Pellissier, Coord. Chem. Rev. 284 (2015) 93–110.
[28] S. Verma, M. Nandi, A. Modak, S.L. Jain, A. Bhaumik, Adv. Synth. Catal. 353 (2011) 1897–1902.
[29] S.L. Jain, B.S. Rana, B. Singh, A.K. Sinha, A. Bhaumik, M. Nandi, B. Sain, Green Chem. 12 (2010) 374–377.
[30] V. Conte, A. Coletti, B. Floris, G. Licini, C. Zonta, Coord. Chem. Rev. 255 (2011) 2165–2177.
[31] F. Farzaneh, Y. Sadeghi, M. Maghami, Z. Asgharpour, J. Clust. Sci. 27 (2016) 1701–1718.
[32] F. Farzaneh, Z. Asgharpour, Appl. Organomet. Chem. (2019), e4896.
[33] S. Bhunia, S. Koner, J. Porous. Mat. 18 (2011) 399–407.